Damage localization map using electromechanical impedance spectrums and inverse distance weighting interpolation: Experimental validation on thin composite structures

Olivier Cherrier, Pierre Selva, Valérie Pommier-Budinger, Frederic Lachaud, Joseph Morlier

Damage localization map using electromechanical impedance spectrums and inverse distance weighting interpolation: Experimental validation on thin composite structures

Olivier Cherrier[1], Pierre Selva[2], Valérie Pommier-Budinger[3], Frédéric Lachaud[1] and Joseph Morlier[1]

Abstract

Piezoelectric sensors are widely used for structure health monitoring technique. In particular, electromechanical impedance techniques give simple and low-cost solutions for detecting damage in composite structures. The purpose of the method proposed in this article is to generate a damage localization map based on both indicators computed from electromechanical impedance spectrums and inverse distance weighting interpolation. The weights for the interpolation have a physical sense and are computed according to an exponential law of the measured attenuation of acoustic waves. One of the main advantages of the method, so-called data-driven method, is that only experimental data are used as inputs for our algorithm. It does not rely on any model. The proposed method has been validated on both one-dimensional and two-dimensional composite structures.

Keywords

Composite structures, damage localization map, electromechanical impedance, inverse distance weighting

Introduction

Structural health monitoring (SHM) is an emerging technology, dealing with the development and implementation of techniques and systems where monitoring, inspection and damage detection become an integral part of structures. It further merges with a variety of techniques that will provide information about the condition of a structure in terms of reliability and safety before the damage threatens the integrity of the structure.[1,2] In the paradigm of SHM, five major steps exist: (a) detection of damage in a structure, (b) localization of damage, (c) damage identification, (d) quantification of damage severity, and (e) prognostic of remaining service life of the structure.[3] SHM systems can be tuned to monitor damage such as fatigue cracks, corrosion, delamination, loose bolts, or impact damage either in real time or on demand. For aeronautical structures, a field where this problem has been quite studied, the components have to resist low-energy impacts caused by dropped tools, mishandling during assembly, and maintenance and in-service impacts by foreign objects such as stones or birds. In these impacts of relative low energy, a small indentation is often referred to as barely visible impact damage (BVID). Although not visually apparent, low-energy impact damage is found to be quite detrimental to the load carrying capabilities of composite structures, underscoring the need of reliable damage detection techniques for composite structures.[4–6] When visual inspection is needed, structural components can be

[1]de Toulouse, Institut Clément Ader, ISAE, UPS, EMAC, INSA, Toulouse, France
[2]Université de Toulouse, ISAE/DMIA, Toulouse, France
[3]ISAE/DMIA, Université de Toulouse, Toulouse, France

Corresponding author:
Valerie Pommier-Budinger, ISAE/DMIA, 10 Avenue Edouard Belin, 31055 Toulouse, France.
Email: valerie.budinger@isae.fr

extracted for maintenance. Successful nondestructive testing (NDT) techniques such as radiographic detection (X-ray) and ultrasound testing (C-Scan) exist but are impractical and/or expensive for large components and integrated vehicles. The major advantage of SHM techniques is their online implementation and their mixed global/local approach (network of sensors).

A promising technique, namely, vibration-based structural health monitoring (VBSHM), has been proposed to address the problem of globally detecting, characterizing, and, to a certain extent, localizing damage based on changes of modal parameters of a structure in operation.[7,8] Any structure can be considered as a dynamic system with stiffness, mass, and damping. Once some damage emerges in the structures, the structural parameters will change, and the frequency response functions (FRFs) and modal parameters of the structural system will also change. This change of modal parameters can be taken as the signal of early damage occurrence in the structural system and especially in composite structures.[9] Recently, some authors[10,11] evaluated experimentally the modal parameter changes due to impacts for several energies of impact. They also demonstrated the sensibility of damping changes to detect delamination in composite structures. Montalvao et al.[12] have succeeded in creating damage localization maps, using three-dimensional (3D) laser vibrometer and an indicator containing information on damping changes and local stress field changes. Friedel et al.[13] proposed a detailed numerical model including the damage pattern obtained from X-ray computed tomographic images. They demonstrated that most of the frequency changes can be explained by one type of damage (delamination) and thus linked the total delamination surface with the absorbed impact energy (affine relation). They built a homogenized damage model, including two damage factors, that allows predicting the change of natural frequencies for a known damage size.

An important research community tries to use local modal parameters such as high-resolution mode shapes (or derived data) to localize damage using wavelet analysis[14–20] or image processing.[21] Finally, another widespread trend is to use, instead of vibration data, high-frequency waves called Lamb waves. Piezoelectric wafer active transducers are used to generate and receive guided Lamb waves propagating in the structure. In the study by Yu and Giurgiutiu,[22] a virtual beam steering method and device used as embedded ultrasonic structural radar was implemented as a signal post-processing procedure. The arrays of piezoelectric transducers (lead zirconate titanate (PZT)) yielded good directionality within the full range of 360° and were able to detect damage anywhere in the entire plate. Ostachowicz et al.[23] also used elastic wave propagation phenomenon from two PZTs for damage detection and localization. As a result of processing of the signals registered from the structure, special maps that indicated damage location on aluminum and composite plates were built. They extended their effort in the study by Malinowski et al.[24] and developed a triangular piezoelectric configuration and an algorithm that transfers information from the time domain to the spatial domain to localize damage on anisotropic material plate.

Classical SHM methods use model-driven data; it means that high-quality models for both undamaged (UD) (baseline) and damaged cases (delamination, crack, etc.) are required. Then, the damage is identified from a metric corresponding to the distance between experimental and numerical data (FRF), natural frequencies, mode shapes, etc.).[25–27] The localization problem can be viewed as an inverse problem often solved using optimization and model updating process[28–32] to minimize the error between experimental and numerical data.

In this article, our approach is mostly experimental. The purpose of our work is based on the following industrial needs:

- Low-cost instrumentation and easy connection;
- Simple criteria for detecting damage;
- Reliable visualization of damage location through signal processing.

To achieve the first point, especially for real-size industrial structures, SHM community often employs smart materials. In particular, the electromechanical impedance (EMI)-based SHM technique possesses distinct advantages such as the ability to detect incipient damage, use of nonintrusive piezoelectric transducers, and potentially low-cost applications.[33–39] A simple method to measure EMIs is the use of an impedance analyzer that allows you to receive information about many electrical quantities (e.g. voltage/current characteristics) as a function of the frequency. In this article, our low-cost SHM system consists of few PZTs (three PZTs for triangulation) that are bonded to the structure and can be plugged to the data acquisition hardware on demand.

For the second point, damage indicators (DIs) derived from the measured EMI are classically used to provide information about damage detection.[39] The earliest works on the EMI method are those published by Liang et al. in two articles.[40,41] The first article presents a coupled electromechanical analysis of piezoelectric ceramic (PZT) actuators integrated in mechanical systems to determine the actuator power consumption and energy transfer in the electromechanical systems. The second article presents the essence of the method with usage of model of piezoelectric transducer bonded to 2-degree-of-freedom structure.

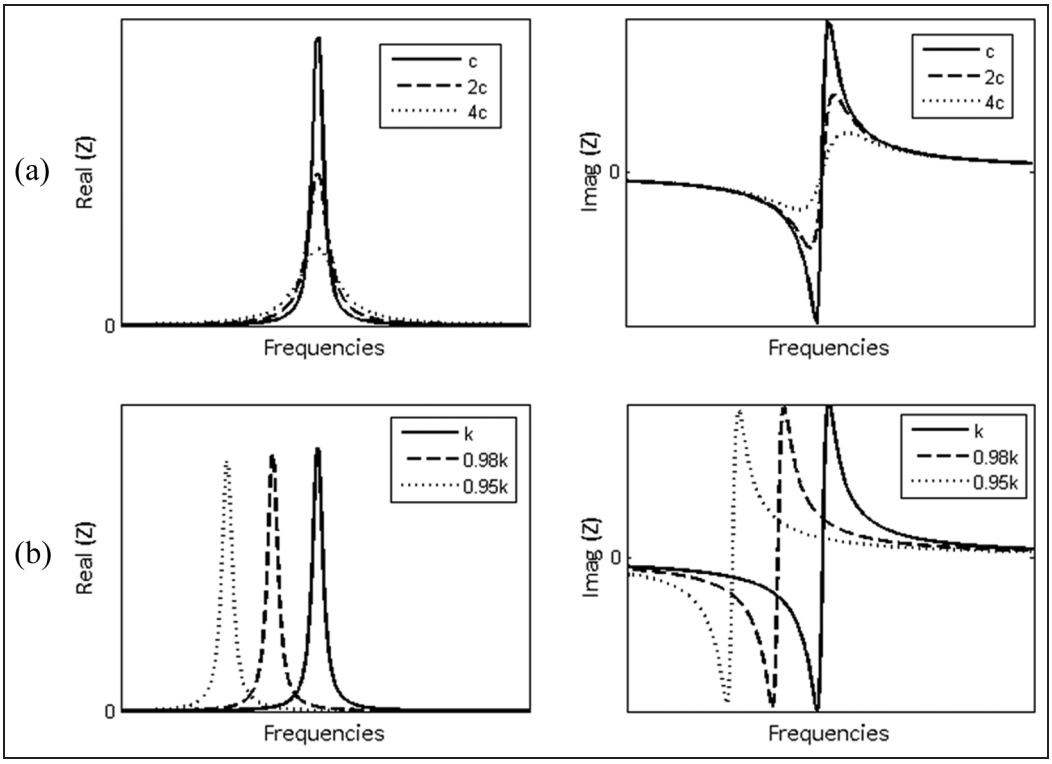

Figure 1. Simple damage model (related to pole shift): (a) example of real and imaginary parts of mechanical impedance versus frequency (a) for an increase in damping coefficients (c, 2c, and 4c) and (b) for a decrease in stiffness (k, 0.98k, and 0.95k).

To achieve the last point and to get reliable localization maps, the analysis of DIs based on EMI is more difficult than the detection. In this article, our original method is based on acoustic wave attenuation and relies on the hypothesis that the interaction between the damaged zone and the sensor depends on the distance between them. Inverse distance weighting (IDW) interpolation will be used to express this hypothesis.

EMI for damage detection

Basics of EMI

The mechanical impedance of a structure, at the force application point, is defined as the ratio of the driving harmonic force to the resulting harmonic velocity at the same point. Thus, the mechanical impedance can be expressed as[36,42,43]

$$Z = R + jX = \frac{F}{v} = \frac{F_0 e^{j\omega t}}{v_0 e^{j(\omega t - \emptyset)}} = \frac{F_0}{v_0} e^{j\emptyset} \qquad (1)$$

where Z is the mechanical impedance, R is the resistance, X is the reactance, F is the force, F_0 is the initial force magnitude, v is the velocity, v_0 is the initial velocity, $\emptyset$ is the phase delay, and ω is the angular frequency.

A continuous structure (such as plate or beam) can be considered as a mass–spring–damper system. Thus, the equivalent mechanical impedance is given by

$$Z_{eq} = \frac{cm^2\omega^2}{c^2 + \left(\omega m - \frac{k}{m}\right)^2} + j\frac{m\omega\left[c^2 - \frac{k}{m}\left(\omega m - \frac{k}{\omega}\right)\right]}{c^2 + \left(\omega m - \frac{k}{\omega}\right)^2} \qquad (2)$$

Damage in laminated composites (delamination due to impact, etc) causes locally an increase in damping and a decrease in stiffness.[7–10] These changes induce a shift in the mechanical impedance. Figure 1 illustrates the effects of these changes on the mechanical impedance spectrum. Figure 1(a) gives an example of real and imaginary parts of a system with three values of the damping coefficient (c, 2c, and 4c). Figure 1(b) gives the real and imaginary parts of a system with three values of the stiffness (k, 0.98k, and 0.95k).

In recent years, the damage detection methods based on the EMI that is a function of the mechanical impedance of a structure have gained increased attention. The methods use small-size piezoelectric transducers intimately bonded to the structure under study. The measured EMI with a piezoelectric transducer is the result of a coupling between the transducer and the structure (Figure 2).

The EMI methods are mostly effective at ultrasonic frequencies, and they properly capture the changes in

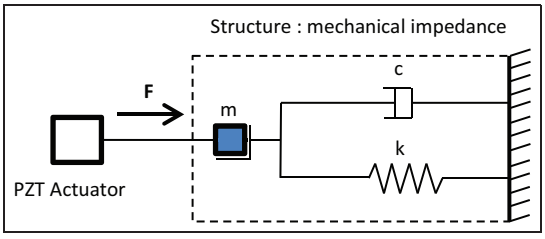

Figure 2. Schematic representation of piezoelectric actuator mounted on an unknown structure.
PZT: lead zirconate titanate.

local dynamics due to incipient structural damage. In complex large structures, such changes are too small to affect the global dynamic behavior of the structure and hence cannot be readily detected by conventional low-frequency vibration methods. Experimental demonstrations have shown that the real part of the high-frequency impedance spectrum is directly affected by the presence of damage or defects in the monitored structure.[42] Besides, a usual bandwidth for thin composite structures is 10–20 kHz.

For detecting damage, the variations of modal parameters have to be estimated with accuracy from the measurement of the EMI. The reliability of the estimation of modal parameters is strongly dependent on several parameters: the sampling frequency, the modal density in the selected bandwidth and also the level of the internal (structural) damping. The real part of the measured impedance is classically used in damage detection because of the simplicity of the process of peak detection.

Damage metrics

The development of suitable damage metrics and damage identification algorithms remains an open question in the practical application of EMI technique. The damage index compares the amplitudes of the two spectrums (damaged vs UD) and assigns a scalar value that serves as a metric for the damage analysis in the structure.[27] In this article, two variation indices (so-called damage features in pattern recognition) are used. The first one is the root mean square deviation (RMSD) and the second is the mean frequency shift of modal peaks (Δf_{mean}).

The RMSD is defined as

$$RMSD(\%) = \sqrt{\frac{\sum_{N}\left[Real(Z_D) - Real(Z_{UD})\right]^2}{\sum_{N}\left[Real(Z_{UD})\right]^2}} \times 100\% \quad (3)$$

where $Real(Z_{UD})$ is the real part of impedance for the UD structure, $Real(Z_D)$ is the real part of impedance for the damaged structure, and N is the number of samples.

The mean frequency shift is defined as

$$\Delta f_{\text{mean}}(\%) = \frac{\sum_{n=1}^{N} \pi \left| f_n^D - f_n^{UD} \right| / f_n^{UD}}{N_{pks}} \times 100\% \quad (4)$$

where f_n^{UD} is the modal frequency of the UD structure for the mode n, f_n^D is the modal frequency of the damaged structure for the mode n, and N_{pks} is the number of modal peaks in the studied frequency band.

These two variation indices can be used for damage detection by comparing their values to thresholds that are significant of damage presence. These thresholds have to be determined experimentally for each structure under study. In this article, we propose to use these indices in a damage localization process by propagating the local information extracted from each sensor to obtain a map of damage.

Damage localization map using acoustic wave attenuation

Acoustic attenuation

Acoustic attenuation is a measure of the energy loss of sound propagation in media and depends on several phenomena (diffraction, reflection, diffusion, and absorption). For laminated materials and unidirectional composite materials, acoustic wave propagation is strongly dependent on fiber spacing and orientation.[44] The technique for measuring the acoustic attenuation coefficient is to evaluate the ratio between incident and transmitted wave levels with an exponential decrease in wave energy[44]

$$\frac{a_t}{a_0} = e^{-m(\omega)x}$$

so

$$m(\omega) = -\frac{\ln(a_t/a_0)}{x} \quad (5)$$

where $m(\omega)$ is the acoustic attenuation coefficient function of the considered frequency, a_0 is the initial level of generated signal (incident wave), and a_t is the received signal after propagation at distance x (transmitted wave). The coefficient used in the next part will be computed from the mean of five measured values. We also observed that for thin composite structures, this coefficient is strongly dependent on the first layer's orientation.

Damage localization map through acoustic attenuation

The main purpose of this article is to construct "damage localization maps" using few piezoelectric

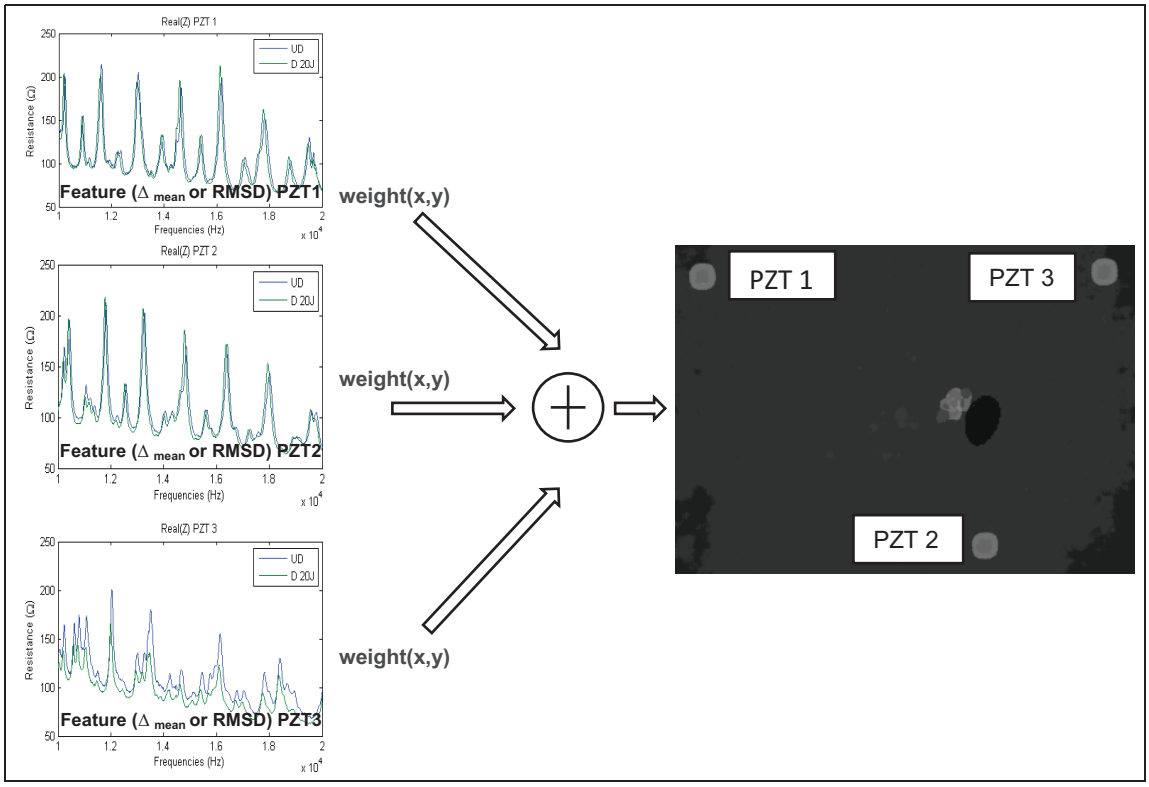

Figure 3. 2D map reconstruction (so-called DI) using the propagation of the three measurements (green points in NDT results). The red area is the SHM damage localization, overlaid of the NDT results (green zone in the center of the plate).
NDT: nondestructive testing; 2D: two-dimensional; DI: damage indicator; SHM: structural health monitoring; RMSD: root mean square deviation; PZT: lead zirconate titanate.

transducers. For example, for a two-dimensional (2D) structure like a plate, three transducers with unsymmetrical position are used to localize damage in the *xy* plane (Figure 3) using the principle of triangulation, which is a method of determining the position of an object by measuring its distance from other objects with known locations. In large structures, the boundary conditions introduce sudden changes in wave propagation, and the method requires to consider the structures as an assembly of several elementary substructures that will all be instrumented. For example, in an aeronautical fuselage, every stiffened panel (or set of panels depending on the accuracy of the damage localization process) is a substructure and needs to be instrumented by three PZTs for triangulation.

Classical triangulation can be conducted on time series for guided waves[45,46] or Lamb waves[47,48] using signal processing tools to enhance the damage map and avoid false damage. The proposed method is based on an enhanced triangulation based on EMI spectrums and weighted DIs. It is inspired from classical IDW interpolation for 2D surface reconstruction of scatter points. IDW methods are based on the assumption that the interpolating surface should be influenced most by the nearby points and less by the more distant points. In the next chapter, our results from online (SHM) methods are compared to those of off-line (NDT) methods in order to prove the accuracy of our SHM-based method.

The proposed method for the construction of damage localization maps can be divided into four steps. Steps 1 and 2 are preliminary steps that are performed once before monitoring. Step 3 is performed continuously. Step 4 is performed only if damage is detected in step 3.

Step 1: instrumentation. Depending on the size of structures, PZT transducers must be chosen large enough in order to give "good" EMI spectrums, that is to say with several modal peaks. They must be bonded with a rigid glue to get a good electromechanical coupling between the transducers and the structure. At least, they must also be bonded to optimal placements that result from a trade-off between requirements for triangulation and EMI measurements.

Step 2: map construction (meshing) using IDW for each piezoelectric transducer. The structure under study is meshed. Obviously, the precision of localization is directly dependent on the mesh size. Each mesh has at least the piezoelectric transducer size.

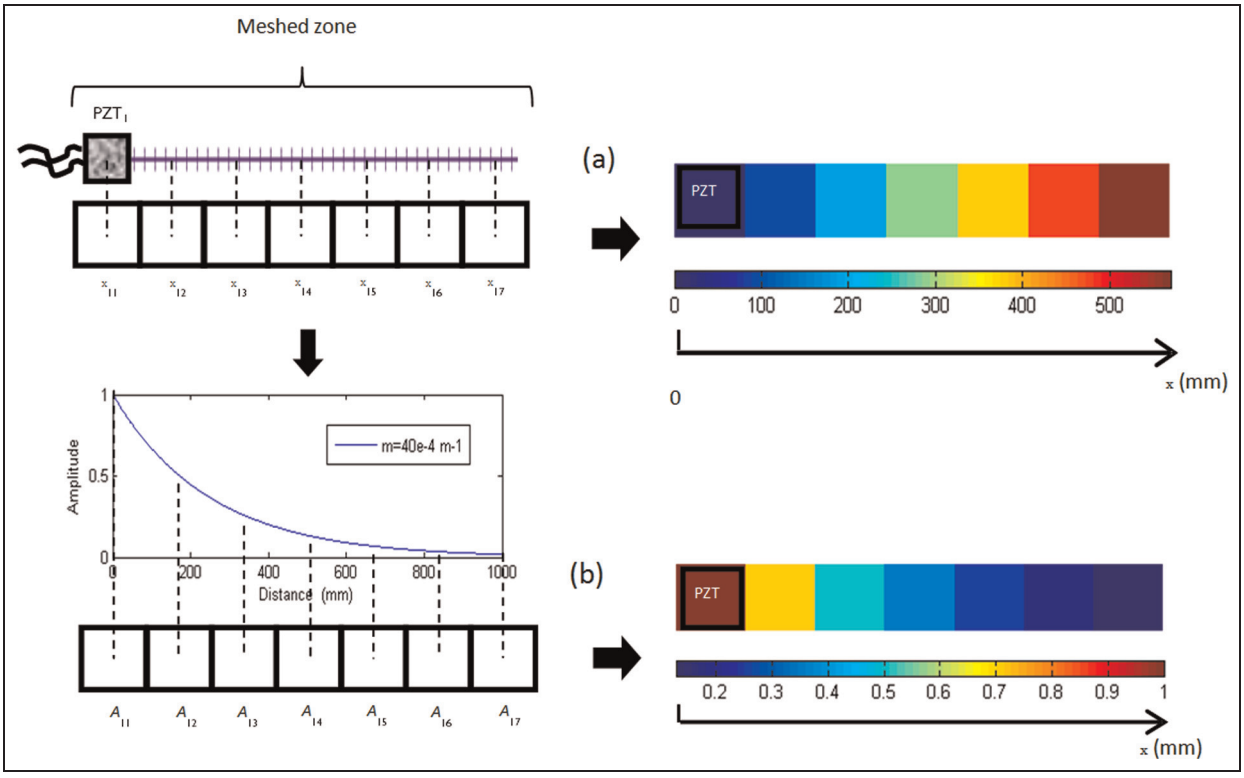

Figure 4. Example of a 1D isotropic structure: (a) mesh in distance and (b) mesh with IDW interpolation computed by the exponential attenuation law for $m = 40e{-}4\ mm^{-1}$.
1D: one-dimensional; IDW: inverse distance weighting; PZT: lead zirconate titanate.

Then, for each transducer denoted as i, every mesh j is weighted by acoustic attenuation A_{ij} defined by

$$A_{ij} = e^{-m(\omega)x_{ij}} \tag{6}$$

where x_{ij} is the distance between the transducer i and the center of each mesh j. Like in IDW methods, the acoustic attenuation is such that it decreases as the distance between the transducer and each scatter point increases.

This method enables to generate weighted maps with a "physical" sense. There are as many weighted maps as transducers.

Step 3: EMI measurements and damage metrics. EMI measurements should be performed regularly for monitoring. In this article, two EMI spectrums are measured for pre and post impact. Then, we can obtain RMSD and Δf_{mean} indices for each transducer using equations (3) and (4). These indices are then compared to thresholds to determine if damage occurs. If yes, a damage localization map is built using step 4 of the method.

Step 4: damage localization map computing. The DIs are computed using IDW interpolation and by taking the inverse in order to get a high value of the indicator in the damaged zone. For each mesh j, the DI based on RMSD index is computed by

$$DI_{j(RMSD)} = \left[\sum_{i=1}^{a}\left(\frac{RMSD_i}{A_{ij}}\right)\right]^{-1} \tag{7}$$

and the DI based on Δf_{mean} index is computed by

$$DI_{j(\Delta f_{\text{mean}})} = \left[\sum_{i=1}^{a}\left(\frac{\Delta f_{\text{mean},i}}{A_{ij}}\right)\right]^{-1} \tag{8}$$

where a is the number of transducers. For one-dimensional (1D) structures, the number of transducers is at least 2, and for 2D structures, it is at least 3. Plotting the values of a DI for each mesh then gives one damage location map that enables to evaluate the damage position on the structure.

Map examples

Figure 4 gives an example of mesh of a 1D structure (Figure 4(a)) and of mesh using IDW interpolation for a sensor located at one extremity (Figure 4(b)).

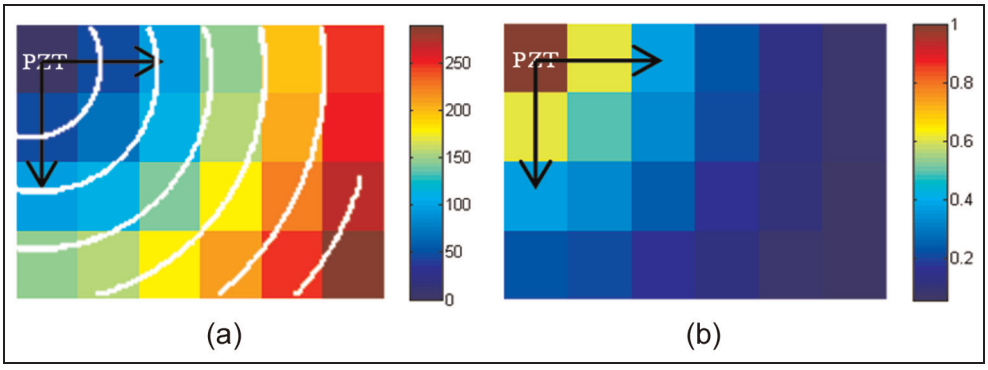

Figure 5. Example of a 2D isotropic structure: (a) mesh in distance and (b) mesh with IDW interpolation computed by the exponential attenuation law for m = 10e−3 mm^{-1} in all directions.
2D: two-dimensional; IDW: inverse distance weighting; PZT: lead zirconate titanate.

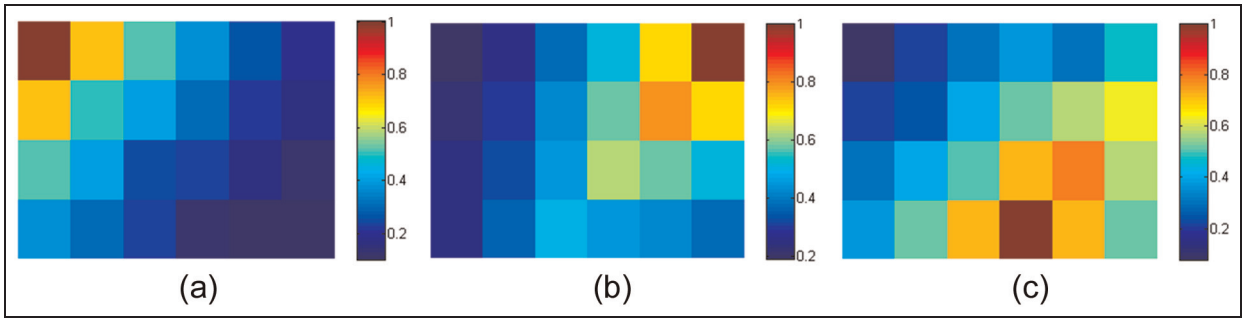

Figure 6. Example of a 2D anisotropic structure—visualization of mesh with IDW interpolation for (a) transducer no. 1, (b) transducer no. 2, and (c) transducer no. 3.
2D: two-dimensional; IDW: inverse distance weighting.

For 2D structures like thin plates, the same concept is carried out in two dimensions. Figure 5 gives an example of mesh of a 2D isotropic plate (Figure 5(a)) and of mesh using IDW interpolation with the same attenuation coefficient in any direction for a sensor located at one extremity.

When the plates are made with unidirectional composite, the mean attenuation must be measured both in fiber direction and in direction transverse to the fibers. Figure 6 gives an example of mesh with IDW interpolation for a thin plate with a mean attenuation equal to 2.8e−3 m^{-1} in the fiber direction and to 10e−3 m^{-1} in the direction transverse to the fibers. The maps are computed for each transducer (three in the studied case) with these coefficients and for a first ply orientation of 45°.

Finally, Figure 7 gives an example of damage localization map. The map is interpolated at higher resolution (×8) for a better visualization (Figure 7(a)). Then, only the zone with the highest probability is plotted to get a single dot and a clear position of damage (Figure 7(b)).

Experimental validation

Case 1: 1D structure (stiffener)

The 1D structure is a composite stiffener of an aircraft door (clamped at the extremities). It has the shape of an I-beam of mean dimensions 66 × 89 × 1045 mm. The beam web is composed of 16 plies of carbon/epoxy plus a peel ply of tissue (considered as equal to isotropic behavior). Two piezoelectric composite patches of type DuraAct® (PI ceramics® PIC255) of dimensions 50 × 30 × 0.5 mm are glued on to the beam web near each extremity of the beam with a structural glue of type 3M DP460® (Figure 8).

A drop test machine is able to create an impact on a specimen with controlled measurements of the impact head (velocity and force) (Figure 9(a)). The chosen target energy is 35 J for each impact because it corresponds to the energy level for which the damage becomes significant but still remains a BVID. Resulting energy is computed from the measured velocity and the mass. Impact data are presented in Table 1. To test the proposed method of impact location, two positions of

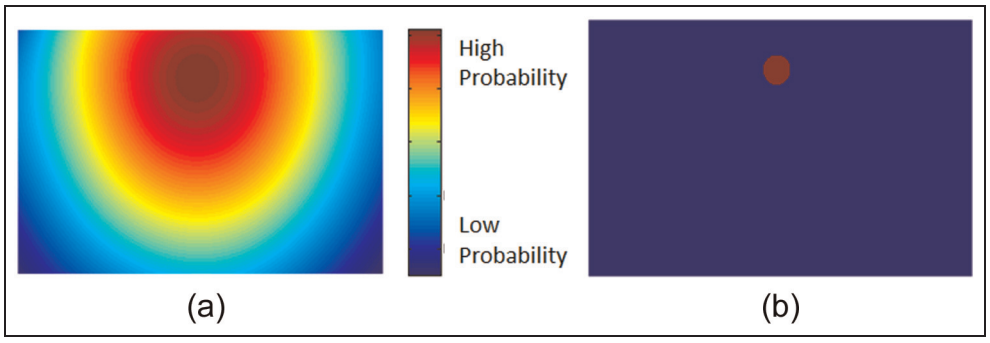

Figure 7. Example of damage localization map for a composite plate (damage located on the top center): (a) Raw DI and (b) processed DI using a threshold that limits the map to higher probability.
DI: damage indicator.

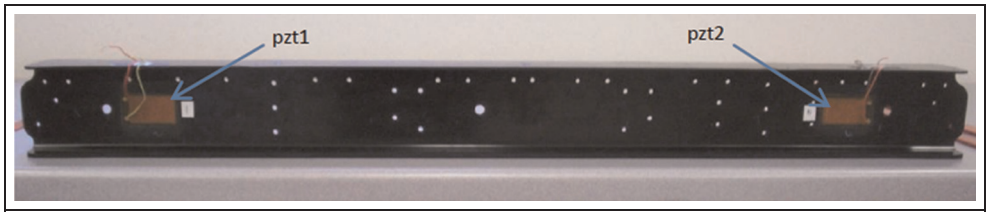

Figure 8. Instrumented composite stiffener, two DuraAct® piezoelectric patches are bonded at the extremities (red zones).

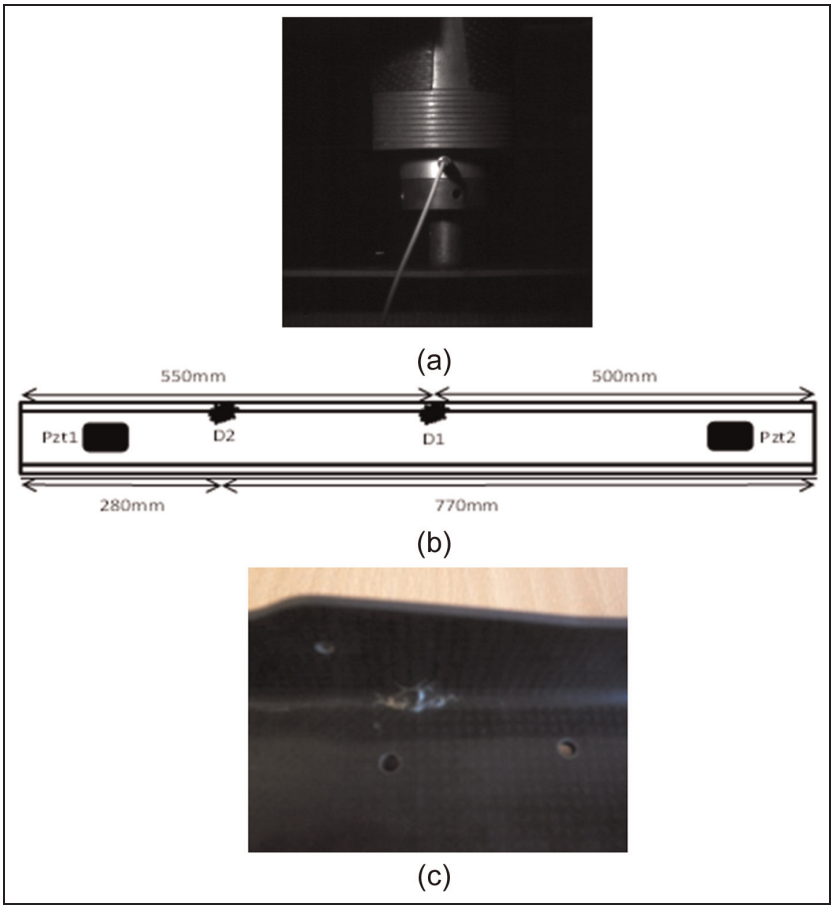

Figure 9. (a) Drop test machine, (b) location of the impacts on the composite stiffener, and (c) example of typical damage.

Table 1. Impact data for the composite stiffener.

	Maximum force (kN)	Mass (kg)	Velocity (m/s)	Target energy (J)	Resulting energy (J)
Impact no. 1	14.5	4	4.25	35	36.2
Impact no. 2	16.8	4	4.3	35	36.9

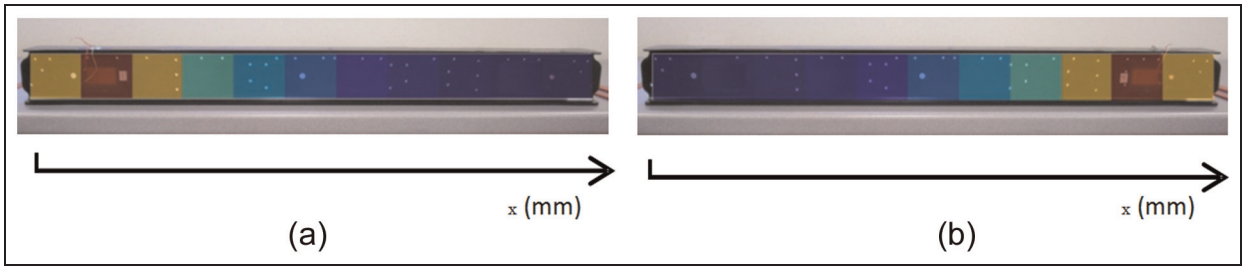

Figure 10. Visualization of mesh with IDW interpolation computed by the exponential attenuation law for $m = 4e{-}3\ m^{-1}$ (a) for transducer no. 1 and (b) for transducer no. 2 in the stiffener case.
IDW: inverse distance weighting.

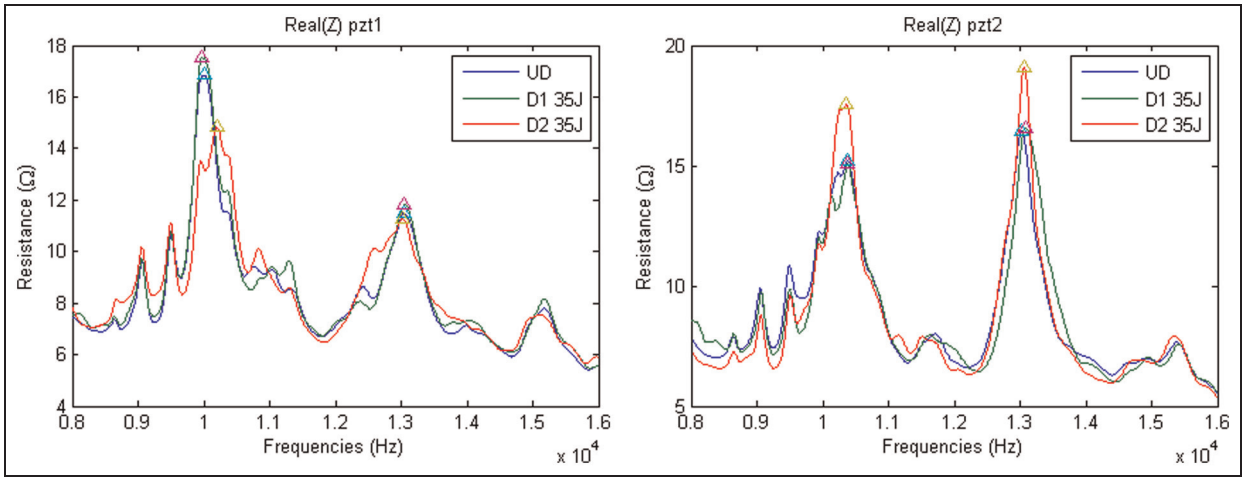

Figure 11. Experimental EMI signatures (between 8 and 16 kHz) for the two transducers on the studied stiffener for UD and damaged cases after a first impact energy of 35 J (D1 = 35 J) and after a second impact energy of 35 J (D2 = 35 J).
UD: undamaged; EMI: electromechanical impedance.

damage between the two transducers are investigated one after the other. Impacts are located on the flange of the beam (Figure 9(b)), and an example of damage is shown in Figure 9(c).

The stiffener web is meshed in equal parts (11 meshes of 95 mm length and 89 mm height). Preliminary tests demonstrate that the best EMI response (i.e. with detectable peaks) is between 8 and 16 kHz for the stiffener. In the beam web, the acoustic attenuation is measured in this frequency band, and the mean value of acoustic attenuation coefficient is $4e{-}3\ m^{-1}$. Then, two maps, one for each transducer, can be computed with IDW interpolation and plotted (Figure 10).

Before and after damage generation, the real part of the EMI is measured (Figure 11). Δf_{mean} and RMSD indices are computed from EMI signatures. The variations of indices are presented in Table 2. Classically, indices for damage no. 2 are computed while considering the state with the first damage as the UD state (D1 replaces UD in equations (3) and (4) as reference).

In Figure 12(a) and (b), the probability of damage is plotted for RMSD. In Figure 12(c) and (d), the results for Δf_{mean} are highlighted. For the first damage, the location predicted by the RMSD index is good since the high-probability zone indicates the real zone of impact.

Table 2. RMSD and Δf_{mean} indices for the composite stiffener and for the two transducers (pzt1 and pzt2).

	$RMSD_{pzt1}$ (%)	$RMSD_{pzt2}$ (%)	$\Delta f_{mean_{pzt1}}$ (%)	$\Delta f_{mean_{pzt2}}$ (%)
Damage no. 1	3.600	8.800	0.180	0.250
Damage no. 2	11.100	11.200	1.210	0.190

RMSD: root mean square deviation.

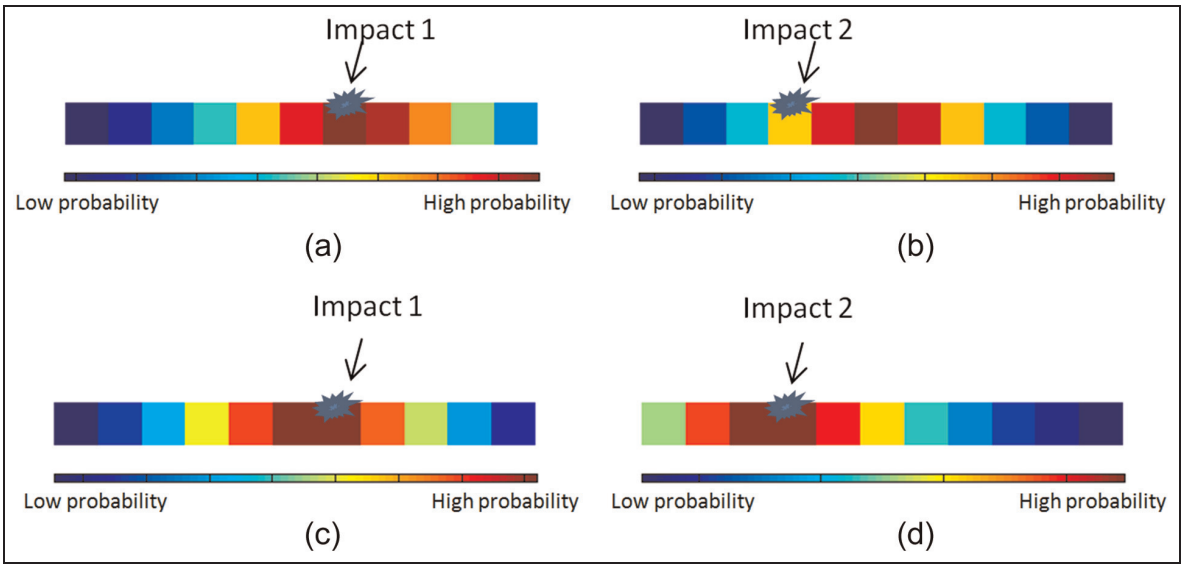

Figure 12. Damage localization maps for the two successive impacts (real in blue circle) for (a, b) RMSD index and for (c, d) Δf_{mean} index.

For the second damage, the predicted location is less accurate. In comparison, the location predicted by the Δf_{mean} index is excellent for every impact.

Case 2: 2D structure (thin composite plates)

Six plates of dimensions 290 × 200 × 3 mm and composed of 12 plies of carbon/epoxy prepreg T700M21 with a stratification [45/-45/0/90/0/90]S for a total thickness of 3 mm are investigated in peripheral clamped configuration (Figure 13). Three PI® PZT piezoelectric ceramics of type PIC151 of dimensions 10 × 10 × 0.5 mm are bonded with structural glue type EPO-TEK® E4110 on each plate as shown in Figure 12.

In this part, six positions of damage are investigated. The chosen target energy is 20 J for each impact, and resulting energy is computed from the measured velocity and force. Impact data are presented in Table 3. In parallel, nondestructive tests (Ultrasonic control C-scans) are carried out to determine the exact position of every impact.

The structure is regularly meshed: 24 meshes of 48 mm length and 50 mm height. Preliminary tests show that the most sensitive EMI signatures are established

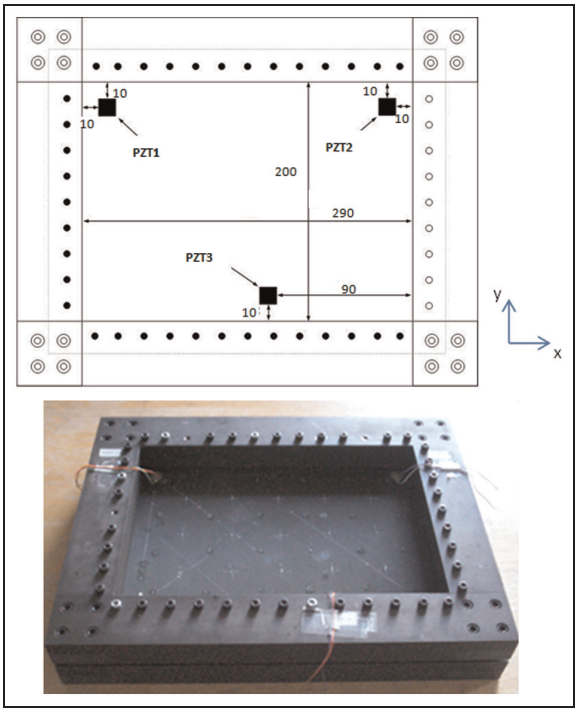

Figure 13. Three piezoelectric transducers bonded to a composite plate in clamped configuration.

Table 3. Impact data for all tested composite plates.

	Maximum force (N)	Mass (kg)	Velocity (m/s)	Target energy (J)	Resulted energy (J)
Plate no. 1	6378.47	2.368	4.100	20	19.90
Plate no. 2	6067.33	2.368	4.095	20	19.85
Plate no. 3	6596.27	2.368	4.118	20	20.08
Plate no. 4	5989.54	2.368	4.095	20	19.85
Plate no. 5	5787.3	2.368	4.010	20	19.00
Plate no. 6	6036.9	2.368	3.996	20	18.90

for the bandwidth 10–20 kHz. The plates have anisotropic behavior, and the mean attenuation must be measured both in fiber direction and in a direction transverse to the fibers. The maps with IDW interpolation computed for each transducer correspond to the ones given as example in Figure 6.

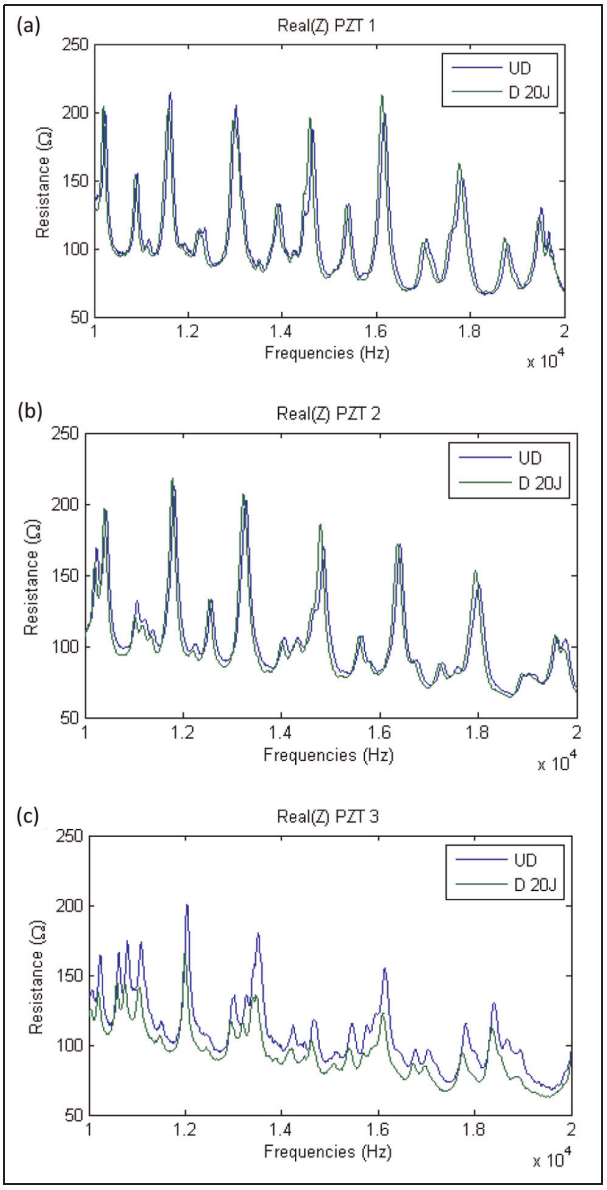

Figure 14. Example of EMI signatures (between 10 and 20 kHz) for the three piezoelectric transducers on the plate no. 1 for UD and damaged cases after an impact energy of 20 J (D = 20 J).
UD: undamaged; EMI: electromechanical impedance.

Table 4. RMSD indices for all tested plates and for every PZT.

RMSD	Plate no. 1	Plate no. 2	Plate no. 3	Plate no. 4	Plate no. 5	Plate no. 6
PZT1	12.99%	8.46%	4.66%	10.15%	14.71%	8.33%
PZT2	13.50%	7.34%	4.35%	11.20%	13.96%	13.51%
PZT3	15.34%	3.93%	10.36%	10.32%	17.76%	12.28%

RMSD: root mean square deviation; PZT: lead zirconate titanate.

Table 5. Δf_{mean} indices for all tested plates and for every PZT.

Δf	Plate no. 1	Plate no. 2	Plate no. 3	Plate no. 4	Plate no. 5	Plate no. 6
PZT1	0.34%	0.20%	0.09%	0.36%	0.69%	0.33%
PZT2	0.38%	0.22%	0.12%	0.33%	0.65%	0.50%
PZT3	0.34%	0.21%	0.12%	0.43%	0.82%	0.51%

PZT: lead zirconate titanate.

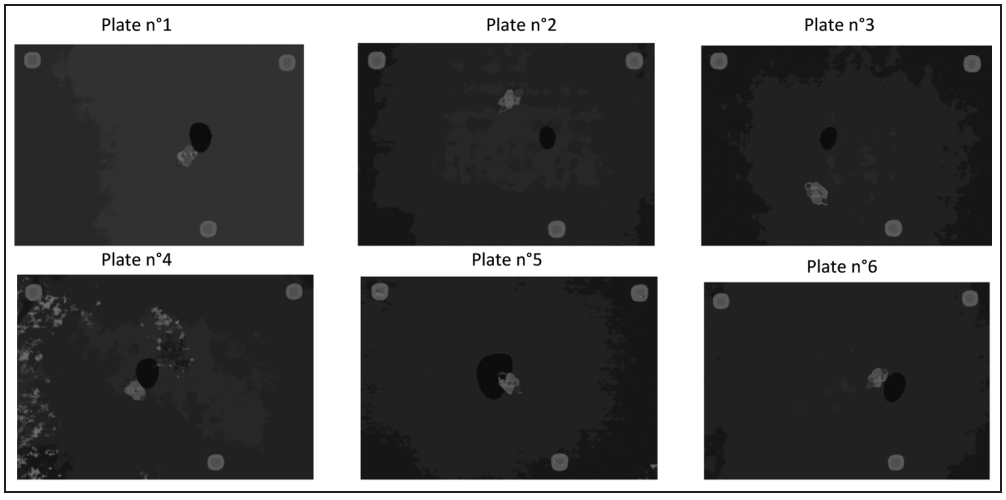

Figure 15. Damage localization maps (Δf_{mean} index) overlaid on Ultrasonic C-scan maps for plate nos 1–6. The DI results (red zone) are compared to NDT test (green zone).
NDT: nondestructive testing; DI: damage indicator.

The real part of the EMI is then measured on every transducer (before and after impact). An example of the EMI signature for plate no. 1 is given in Figure 14. Using all EMI signatures, Δf_{mean} and RMSD indices can be computed for every plate (Tables 4 and 5).

The damage localization maps are finally computed for both variation indices. The maps in Figures 15 and 16 are overlaid for comparison with the Ultrasonic control C-scans. Both indices permit to give a good estimation of damage localization. Maximal errors are less than the damage size (typically around 20 mm), but in this case, RMSD is more reliable.

Conclusion

The proposed method permits to detect and localize a single isolated damage in composite structures. Piezoelectric transducers bonded to the structure enable to measure EMIs. The purpose of the method in this article is to generate a damage localization map based on both indicators computed from EMI spectrums and IDW interpolation. The weights for the interpolation have a physical sense and are computed according to an exponential law of the measured attenuation of acoustic waves. One of the main advantages of our

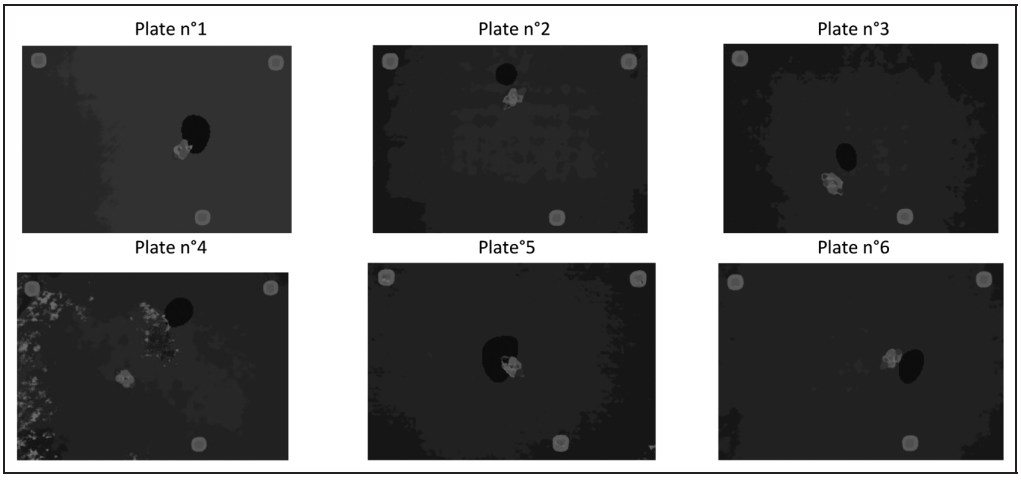

Figure 16. Damage localization maps (RMSD indices) overlaid on Ultrasonic C-scan maps for plate nos 1–6. The DI results (red zone) are compared to NDT test (green zone).
NDT: nondestructive testing; DI: damage indicator; RMSD: root mean square deviation.

method, so-called data-driven method, is that only experimental data are used as inputs for our algorithms. It does not rely on any model. The proposed method has been validated in both 1D and 2D composite structures. Future works will consist in evaluating damage severity through an updating process based on gradient optimization. These works will naturally lead to a comparison of our data-driven method to model-driven method based on high-fidelity finite element (FE) models and supervised learning (probabilistic neural networks (PNN)). Other perspectives to improve the method are to consider more than three transducers for each substructure in order to carry out several damage localization analyses with sets of three transducers and then to compare the results of each set to avoid false damage detection and to increase the reliability.

Acknowledgements

The authors thank N. Boudjemaa, LATECOERE, for his insightful comments.

Declaration of conflicting interests

The authors declare that there is no conflict of interest.

Funding

This study received financial support from the Région Midi-Pyrénées, the DIRRECTE as well as the FEDER through EPICEA 2009 program related to the project titled "SAPES COMPOSITES."

References

1. Farrar CR and Worden K. An introduction to structural health monitoring. *Philos T R Soc A* 2007; 365: 303–315.
2. Doebling SW, Farrar CR and Prime MB. A summary review of vibration-based damage identification methods. *Shock Vib Digest* 1998; 30: 91–105.
3. Farrar CR and Lieven AJ. Damage prognosis: the future of structural health monitoring. *Philos T R Soc A* 2007; 365: 623–632.
4. Schubel PM, Luo JJ and Daniel IM. Impact and post impact behaviour of composite sandwich panels. *Composites Part A: Appl S* 2007; 38: 1051–1057.
5. Abrate S. *Impact on composite structures*. Cambridge: Cambridge University Press, 1998.
6. Petit S, Bouvet C, Bergerot A, et al. Impact and compression after impact experimental study of a composite laminate with a cork thermal shield. *Compos Sci Technol* 2007; 67: 3286–3299.
7. Cawley P and Adams RD. The location of defects in structures from measurements of natural frequencies. *J Strain Anal Eng* 1979; 14(2): 49–57.
8. Farrar CR, Doebling SW and Nix DA. Vibration-based structural damage identification. *Philos T R Soc A* 2001; 359(1778): 131–149.
9. Montalvão D, Maia NMM and Ribeiro AMR. A review of vibration-based structural health monitoring with special emphasis on composite materials. *Shock Vib Digest* 2006; 38(4): 295–324.
10. Shahdin A, Morlier J and Gourinat Y. Correlating low energy impact damage with changes in modal parameters: a preliminary study on composite beams. *Struct Health Monit* 2009; 8(6): 523–536.
11. Shahdin A, Morlier J and Gourinat Y. Damage monitoring in sandwich beams by modal parameter shifts: a comparative study of burst random and sine dwell vibration testing. *J Sound Vib* 2010; 3(5): 566–584.
12. Montalvao D, Ribeiro AM and Duarte-Silva J. A method for the localization of damage in a CFRP plate using damping. *Mech Syst Signal Pr* 2008; 23(6): 1846–1854.

13. Frieden J, Cugnoni J, Botsis J, et al. Vibration-based characterization of impact induced delamination in composite plates using embedded FBG sensors and numerical modelling. *Compos Part B: Eng* 2011; 42(4): 607–613.
14. Morlier J, Bos F and Castera P. Diagnosis of a portal frame using advanced signal processing of laser vibrometer data. *J Sound Vib* 2006; 297(1–2): 420–431.
15. Rucka M and Wilde K. Application of continuous wavelet transform in vibration based damage detection method for beams and plates. *J Sound Vib* 2006; 297(3–5): 536–550.
16. Kim BH, Kim H and Park T. Nondestructive damage evaluation of plates using the multiresolution analysis of two-dimensional Haar wavelet. *J Sound Vib* 2006; 292(1–2): 82–104.
17. Huang Y, Meyer D and Nemat-Nesser S. Damage detection with spatially distributed 2D continuous wavelet transform. *Mech Mater* 2009; 41(10): 1096–1107.
18. Loutridis S, Douka E, Hadjileontiadis L, et al. A two-dimensional wavelet transform for detection of cracks in plates. *Eng Struct* 2005; 27(9): 1327–1338.
19. Fan W and Qiao P. A 2-D continuous wavelet transform of mode shape data for damage detection of plate structures. *Int J Solids Struct* 2009; 46(25–26): 4379–4395.
20. Katunin A. Damage identification in composite plates using two-dimensional B-spline wavelets. *Mech Syst Signal Pr* 2011; 25(8): 3153–3167.
21. Morlier J and Mevel L. Modeshapes recognition using Fourier descriptors: a simple SHM example. In: *Proceedings of the 30th international modal analysis conference (IMAC-XXX)*, Jacksonville, FL, 30 January–2 February 2012.
22. Yu L and Giurgiutiu V. In situ 2-D piezoelectric wafer active sensors arrays for guided wave damage detection. *Ultrasonics* 2008; 48(2): 117–134.
23. Ostachowicz W, Kudela P, Malinowski P, et al. Damage localisation in plate-like structures based on PZT sensors. *Mech Syst Signal Pr* 2009; 23(6): 1805–1829.
24. Malinowski P, Wandowski T and Ostachowicz W. Damage detection potential of a triangular piezoelectric configuration. *Mech Syst Signal Pr* 2011; 25(7): 2722–2732.
25. Adams DE. *Health monitoring of structural materials and components*. Chichester: John Wiley & Sons Ltd, 2007.
26. Staszewski WJ, Boller C and Tomlinson GR. *Health monitoring of aerospace structures*. Chichester: John Wiley & Sons Ltd, 2003.
27. Worden K, Farrar CR, Manson G, et al. The fundamental axioms of structural health monitoring. *P Roy Soc A: Math Phy* 2007; 463(2082): 1639–1664.
28. Moaveni B, He X and Conte JP. Damage identification of a composite beam using finite element model updating. *Comput-Aided Civ Inf* 2008; 23(5): 339–359.
29. Meo M and Zumpano G. Damage assessment on plate-like structures using a global-local optimization approach. *Optim Eng* 2008; 9(2): 161–177.
30. Niemann H, Morlier J, Shahdin A, et al. Damage localization using experimental modal parameters and topology optimization. *Mech Syst Signal Pr* 2010; 24(3): 636–652.
31. Shahdin A, Morlier J, Niemann H, et al. Correlating low energy impact damage with changes in modal parameters: diagnosis tools and FE validation. *Struct Health Monit* 2011; 10(2): 199–217.
32. Viana JC, Antunes PJ, Guimara RJ, et al. Combining experimental and computed data for effective SHM of critical structural components. In: *IEEE aerospace conference*, Big Sky, MT, 5–12 March 2011, pp. 1–10.
33. Park G, Sohn H, Farra CR, et al. Overview of piezoelectric impedance-based health monitoring and path forward. *Shock Vib Digest* 2003; 35(5): 451–463.
34. Lim Y, Bhalla S and Soh CK. Structural identification and damage diagnosis using self-sensing piezo-impedance transducers. *Smar Mat St* 2006; 15(4): 987–995.
35. Yan W, Cai JB and Chen WQ. Monitoring interfacial defects in a composite beam using impedance signatures. *J Sound Vib* 2009; 326(1–2): 340–352.
36. Bhalla S and Soh CK. Structural health monitoring by piezo-impedance transducers applications. *J Aerospace Eng* 2004; 17(4): 166–175.
37. Yan W and Chen WQ. Structural health monitoring using high-frequency electromechanical signatures. *Adv Civil Eng* 2010.
38. Bhalla S, Gupta A and Bansal S. Ultra low-cost adaptations of electro-mechanical impedance technique for structural health monitoring. *J Intel Mat Syst Str* 2009; 20(8): 991–999.
39. Giurgiutiu V and Zagrai A. Damage detection in thin plates and aerospace structures with the electro-mechanical impedance method. *Struct Health Monit* 2005; 4(9): 1025–1036.
40. Liang C, Sun FP and Rogers CA. Coupled electro-mechanical analysis of adaptative systems—determination of the actuator power consumption and system energy transfer. *J Intel Mat Syst Str* 1994; 5(1): 12–20.
41. Liang C, Sun FP and Rogers CA. An impedance method for dynamic analysis of active material system. *J Vib Acoust* 1994; 116(1): 120–128.
42. Giurgiutiu V. *Structural health monitoring with piezoelectric wafer active sensors*. New York: Elsevier Academic Press, 2008.
43. Bhalla S and Soh C. Structural health monitoring by piezo-impedance transducers part I: modeling. *J Aerospace Eng* 2004; 17(4): 154–165.
44. Williams JH, Nayeb-Hashemi J and Lee SS. *Ultrasonic attenuation and velocity in AS3501-6 graphite/epoxy fiber composite*. *J Nondestruct Eval* 1980; 1(2): 137–148.
45. Flynn EB, Todd MD, Dunn CT, et al. Identifying scatter targets in 2D space using in situ phased-arrays for guided wave structural health monitoring. In: *Proceedings of the 8th international workshop on structural health monitoring*, Stanford University, Stanford, CA, 12–15 September 2011.
46. Kessler SS, Flynn EB, Dunn CT, et al. A structural health monitoring software tool for optimization, diagnostics and prognostics. In: *Proceedings of the 3rd annual conference of the prognostics and health management society*, Montreal, QC, Canada, 25–29 September 2011.
47. Chao Z, Su Z and Cheng L. Quantitative evaluation of orientation-specific damage using elastic waves and probability-based diagnostic imaging. *Mech Syst Signal Pr* 2011; 25(6): 2135–2156.
48. Su Z and Ye L. *Identification of damage using Lamb waves: from fundamentals to applications*. London: Springer, 2009.